Publication III

H. Rimminen, J. Lindström, and R. Sepponen. 2009. Positioning accuracy and multi-target separation with a human tracking system using near field imaging. International Journal on Smart Sensing and Intelligent Systems, volume 2, number 1, pages 156-175.

POSITIONING ACCURACY AND MULTI-TARGET SEPARATION WITH A HUMAN TRACKING SYSTEM USING NEAR FIELD IMAGING

H. Rimminen[1], J. Lindström[2], and R. Sepponen[1]

[1]Department of Electronics, Helsinki University of Technology, Otakaari 7 B, Espoo, Finland.

[2]Elsi technologies Ltd, Kimmeltie 3, Espoo, Finland.

Emails: henry.rimminen@tkk.fi, juha.lindstrom@elsi.fi, raimo.sepponen@hut.fi

Abstract - We analyze the performance of a novel human tracking system, which uses the electric near field to sense human presence. The positioning accuracy with moving targets is measured using raw observations, observation centroids and Kalman filtered centroids. In addition to this, the multi-target discrimination performance is studied with two people and a Rao-Blackwellized Monte Carlo data association algorithm. A reel-based triangulation system is used as the reference positioning system. The mean positioning error for five test subjects walking at different speeds is 21 centimeters. The discrimination performance is 90% when the distance between the two people is over 0.8 meters. With distance over 1.1 meters the discrimination performance is 99%.

Index terms*:* Floor sensor, Near field imaging, Human tracking, Multiple target tracking.

I.   INTRODUCTION

This study analyzes the performance of a novel human tracking system called the Electronic Sensor with Intelligence (ELSI). It senses the presence of human beings using an electric near field [1] and we refer to this method as near field imaging (NFI). A similar method for human detection was first published by Zimmerman [2] in 1995. The sensor system under study here can also record the vital signs of a fallen person [3] and is able to detect falls. The electric field is produced by a conductive film array under the floor surface. The floor may be covered with arbitrary dielectric material up to 10 millimeters thick, which makes the system completely undetectable. In addition to this, the amount of floor area covered with the sensor system is unlimited.

The main application of the NFI floor sensor is monitoring residents in homes for the elderly and monitoring elderly people at home. The rapid ageing of the population in the EU [4] is creating pressure to make the elderly care system more efficient. This can be partly achieved with an advanced monitoring solution such as ELSI, since the availability of qualified staff for nursing homes is very limited as it is. In addition to this, the possibility of remote monitoring may enable elderly people to live at home for extended periods, lowering the costs inflicted on society.

In homes for the elderly the NFI system would be used for triggering alarms, such as exiting/entering the room, getting out of/into bed, or entering/exiting the toilet, which all require accurate tracking. At home the NFI system would provide information about the overall health of the person. It has been proposed that the functional health status of the elderly could be determined remotely by measuring simple parameters such as mobility, sleep patterns, and the utilization of cooking, washing, and toilet facilities [5]. Measuring these parameters with the NFI system is possible but requires tracking.

Remote monitoring of the elderly with multiple sensors in their homes has already been found to slightly increase their quality of life and significantly lower the strain on the caregivers [6].

a. State of the art

Human tracking can be performed with many types of hardware: with ultrasound [7]; with infrared light [8]; with radio frequencies [9], [10], [11]; with computer vision [12], [13], and by floor contact sensing [14], [15], [16]. The motivation of an NFI system is to avoid some major disadvantages found in other tracking hardware. There is no need to carry a transponder, such as with ultrasonic, infrared or RF-based systems, and the accuracy of NFI is more than eight times better compared to RF-based tracking systems. The performance is not hindered by changes in the background or lighting, and no intimacy issues arise, in contrast to camera-based tracking. The other floor sensors found in the literature are based on weight sensing, which requires a very complex floor structure compared to the glue-on films of the NFI method.

One very promising study focusing on floor sensor tracking was carried out by Murakita [17], whose scope is very similar to ours, but the discrete floor sensors caused the system to miss observations when the weights of the test subjects varied. This potentially limited the accuracy of their system. The non-discrete observation strengths of our tracking system are not proportional to weight, but to the intersecting area of the activated sensor cell and the foot of the target. This

adds more information to the observations and makes them immune to the weight of the target. In addition to this, the reference positioning system used in this study is unique and very accurate; we do not have to make assumptions about the actual location or speed of the target, such as that the target is walking exactly on a defined path and maintaining uniform speed.

b. Tracking people with NFI

Usually a human target activates at least two sensor cells - one cell for each foot. When monitoring a standing person, the coordinates of the activated sensors weighted by the signal strengths (i.e. the centroid of the observations) is a good approximation for the location of the person because it is usually somewhere between the feet. A walking person produces a more complex observation pattern as the advancing foot usually moves high leaving the supporting foot to contribute to the observations alone. The observation centroid remains at the supporting foot until the advancing foot touches the floor. This makes the observation centroid a rather noisy estimator for the location. A tracking algorithm can filter some of the noise and improve the positioning accuracy. A tracking algorithm can also predict the location for example when some observations are lost.

When there are two or more targets, each observation has to be associated with the correct target before the location estimate can be updated. If the targets are close to each other, this is not trivial because of the relatively low resolution of the NFI sensor matrix. In the tracking community this is known as the data association problem and there are sophisticated algorithms for attacking it.

c. Goals of the study

Our goal was to measure the real-time positioning accuracy of our floor sensor system using moving human targets. We also aimed to measure the real-time multi-target separation performance using two people. The reference location of the targets was to be acquired with a high-precision reference tracking system, which we fabricated for this purpose.

II.   MATERIALS AND METHODS

a. The reference tracking system

To be able to measure the positioning accuracy of the NFI tracking system, we need a rugged and accurate reference positioning system. For this purpose, a reel-based triangulation system was built, using precision potentiometers and multifiber fishing lines; see figure 1. The reels have rotary carved spools in them, which are attached to the framework with ball bearings. The spools have two grooves on them with different diameters. One is for the flat cord of a retractable dog leash. This adds a spring-loaded turning motion to the spool. The other groove on the spool is for the actual fishing line (PowerPro, 0.36 mm DIA., Innovative Textiles, Inc., Grand Junction, CO). The diameter of this groove is defined in such a way that the diagonal length of the test room can be reached by using only ten whole turns of the spool. The amount of turns is limited by the structure of the precision potentiometers (8146R1KL.25, BI Technologies Corp., Fullerton, CA).

Figure. 1. The triangulation reference reel and the positioning hat. Retractable dog leashes are used to achieve the retracting motion of the positioning lines. The ten-turn precision potentiometer used is visible under the spool on the right.

The three reels are located in the top corners of the test room, which has the NFI sensors installed under the floor surface. The test subject walks on the sensor floor wearing a tight-fitting hat with the three lines attached on top of it; see figure 2 for the test configuration. Because the reels are placed in three corners of a rectangular room, the position of the hat can be solved with simple

trigonometry. Calibration is needed only once. This is done by measuring the slacks of the reels when the potentiometers read zero, and counting these values into the calculations.
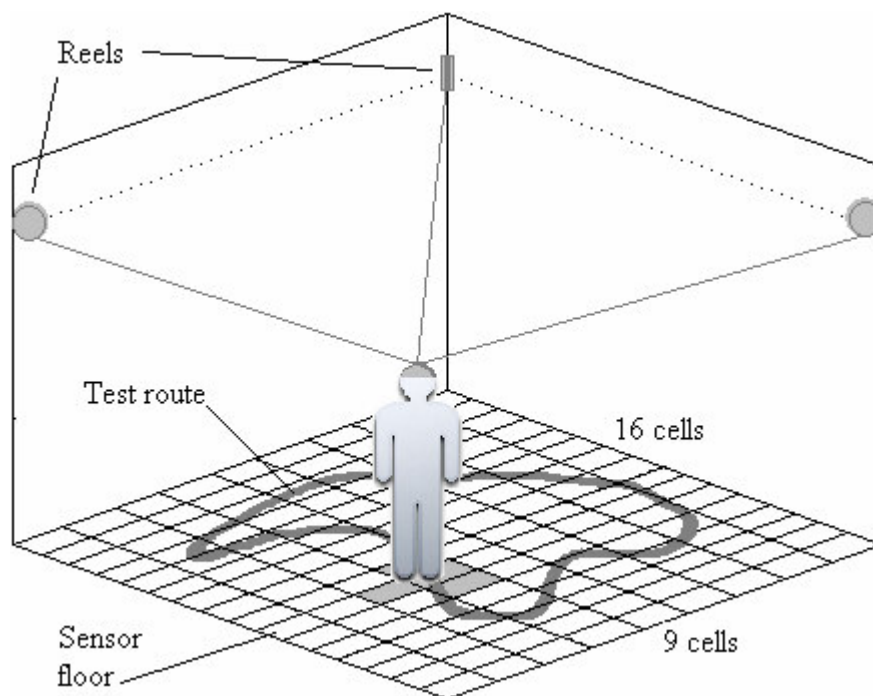
Figure 2. The test configuration. Floor sensor resolution is 0.5 m x 0.25 m, and area size is 4.5 m x 4 m. Positioning reels are placed in three corners of the room.

To verify the positioning accuracy of the triangulation system, a series of measurements are performed using a measuring tape: the node of the three lines is placed in ten different positions on the floor, and the corresponding tape measurements are compared with the results given by the triangulation system. The goal is to achieve a positioning accuracy and update rate at least one decade higher than that achieved with the NFI floor sensor. The floor sensor observation resolution is 50 cm x 25 cm, and the update rate is approximately 5 updates per second.

After the reference system has been verified, observation data and reference data can be acquired. The test subjects walk along an arbitrary taped route on the floor wearing the positioning hat and their own shoes. Everyone in the group walks the same route. The test group consists of five people, three males and two females. Each of them walks a total of nine laps, increasing their walking speed after every three laps: they are first asked to walk slowly, then at a medium speed, and finally at a fast speed. The length of the taped route is approximately ten meters.

b. Position estimation

For the sensor system to be useful in tracking people, we have to be able to estimate the position of the subject from the sensor observations. The question is what kind of an estimator gives the most accurate estimates. We can compare different estimators by comparing their output to the reference estimate given by the reference tracking system. Statistics of particular interest are the mean and the standard deviation of the error, i.e. the difference between the reference tracking system and the estimator under evaluation.

A naïve estimator could just pick the strongest observation and use the location of the corresponding sensor as the position estimate. Obviously this estimator cannot be very good, as it just discards the information available in the other observations and restricts the estimate to a discrete set of sensor locations. Nevertheless, it serves as an interesting baseline.

Typically, a person standing or walking on the sensor floor causes activation in multiple sensors. We assume that the strength of the signal from one sensor is proportional to the intersecting area between the sensor cell and the foot of the subject. This intersection forms a parallel-plate capacitor insulated by the floor covering and the more or less uniform shoe sole; see the gray areas in figure 3. This assumption is completed by the linear impedance sensitivity of the system, which has been shown earlier [1]. Therefore, a natural way to use multiple observations is to compute the centroid of the observation cluster, as in (1). The position estimate $[x_C, y_C]$ is the average position of the activated sensors $[x_i, y_i]$ weighted by the strength of the observations ΔZ_i.

$$x_C = \frac{\sum_{i=1}^{N} \Delta Z_i x_i}{\sum_{i=1}^{N} \Delta Z_i}, y_C = \frac{\sum_{i=1}^{N} \Delta Z_i y_i}{\sum_{i=1}^{N} \Delta Z_i} \qquad (1)$$

The position estimate given by the centroid estimator is expected to contain errors resulting from differences in the sensor film gaps, shoes, and target posture, among other things. Observations can also be lost momentarily. Therefore, especially for a moving target, it makes sense to try to filter this estimate to reduce the noise caused by these errors.
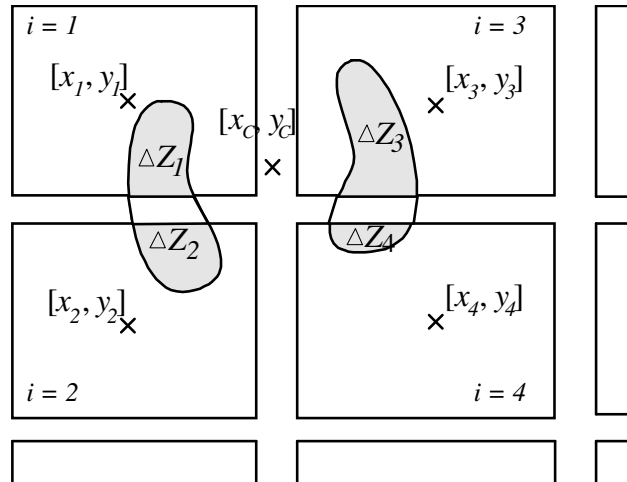
Figure 3. The definition of the observation centroid (x_c and y_c). Gray areas represent the intersections of sensor cells and feet. The detected impedance changes ΔZ_i are proportional to these areas. Here the centroid consists of four sensor observations (i goes from 1 to 4).

c. Kalman filter

The Kalman filter is an efficient recursive filter that estimates the state of a linear dynamic system from a series of noisy measurements [18]. It can be seen as a special case of a more general Bayesian filtering framework that is often used in tracking problems [19]. The Kalman filter requires the state of the system to evolve linearly and the noises present in the system and the measurements to be white and Gaussian.

In order to apply the Kalman filter to our tracking problem, we chose to model the state of a walking person using a simple continuous white noise acceleration (CWNA) model [20]. In this model, the acceleration of the target is assumed to be a zero-mean Gaussian white noise process and therefore the expected velocity of the target is constant. While this limited model does not reflect the reality very accurately, it is difficult to come up with a better model, if we cannot assume anything about the path of the target.

In the CWNA model the continuous-time state equation for the target is (3)

$$\frac{d^2\mathbf{x}(t)}{dt^2} = \mathbf{w}(t),\qquad(3)$$

where the target state $\mathbf{x}(t) = [x(t), y(t)]^T$ is the position of the target at time t. The zero mean Gaussian white noise process $\mathbf{w}(t)$ with spectral density q represents random fluctuations in the acceleration of the target. The equivalent discrete-time state equation is (4)

$$\mathbf{x}_k = \mathbf{A}_k \mathbf{x}_{k-1} + \mathbf{q}_k, \qquad (4)$$

where the target state $\mathbf{x}_k = [x_k, y_k, \dot{x}_k, \dot{y}_k]$ consists of the position and the velocity of the target at time t_k. The old state of the target $\mathbf{x}_{k-1}$ is mapped to the new state $\mathbf{x}_k$ using the linear state transition model $\mathbf{A}_k$. The process noise $\mathbf{q}_k$ is assumed to be drawn from a zero mean multivariate normal distribution with covariance $\mathbf{Q}_k$. The transition model $\mathbf{A}_k$ and the process noise covariance $\mathbf{Q}_k$ are given in (5)

$$\mathbf{A}_k = \begin{bmatrix} 1 & 0 & \Delta t_k & 0 \\ 0 & 1 & 0 & \Delta t_k \\ 0 & 0 & 1 & 0 \\ 0 & 0 & 0 & 1 \end{bmatrix}, \quad \mathbf{Q}_k = q \begin{bmatrix} \frac{\Delta t_k^3}{3} & 0 & \frac{\Delta t_k^2}{2} & 0 \\ 0 & \frac{\Delta t_k^3}{3} & 0 & \frac{\Delta t_k^2}{2} \\ \frac{\Delta t_k^2}{2} & 0 & \Delta t_k & 0 \\ 0 & \frac{\Delta t_k^2}{2} & 0 & \Delta t_k \end{bmatrix}, \quad (5)$$

where q is the spectral density of the process noise $\mathbf{w}(t)$ and Δt_k is the time between time steps k and $k-1$.

Since our observations are the centroids of the actual measurements, we can define the observation model for our Kalman filter as (6)

$$\mathbf{z}_k = \mathbf{H}_k \mathbf{x}_k + \mathbf{v}_k, \qquad (6)$$

where $\mathbf{z}_k$ is the location of the measurement centroid at time step k and the 2-by-4 matrix $\mathbf{H}_k$ maps the state of the target $\mathbf{x}_k$ to the location of the centroid. The measurement noise $\mathbf{v}_k$ corresponds to the error between the location of the centroid and the location of the target. As required by the Kalman filter, it is assumed to be white and drawn from a zero mean multivariate normal distribution with constant covariance $\mathbf{R}$. In reality, while the distribution of the noise is

quite normal, consecutive samples do have some correlation and hence the noise is not quite white. The observation model matrix $\mathbf{H}_k$ simply picks the location of the target from the state vector and is defined as in (8)

$$\mathbf{H}_k = \begin{bmatrix} 1 & 0 & 0 & 0 \\ 0 & 1 & 0 & 0 \end{bmatrix}. \qquad (8)$$

The model parameters $\mathbf{R}$ and q were tuned using a separate training set of samples from the sensor floor and the reference positioning system. Two test subjects were used as the training set. Only the slow and medium walking speed samples were used for training purposes because otherwise the process noise would have been too high.

Since there is no reason why the x and y dimensions of the observations should have any correlation, we assumed that the measurement noise covariance $\mathbf{R}$ matrix is diagonal and can be directly estimated from the training set using (9)

$$\mathbf{R} = \frac{1}{N-1} \begin{bmatrix} \sum_{i=1}^{N} \Delta x_i^2 & 0 \\ 0 & \sum_{i=1}^{N} \Delta y_i^2 \end{bmatrix}, \qquad (9)$$

where N is the size of the training set and Δx_i and Δy_i are the differences between the position of the centroid and the corresponding actual position given by the reference system.

Estimating the spectral density q of the process noise $\mathbf{w}(t)$ in (3) from the training set is not as straightforward, since the reference system does not measure velocity or acceleration directly. We would first need to estimate them from the position measurements and that would introduce additional errors. Therefore, we chose to simply numerically optimize the value of q so that it minimizes the mean estimation error of the Kalman filter within the training set.

e. Multiple target tracking

Since our reference tracking system can only track one person at a time, we had to resort to a special method in order to evaluate the tracking performance of the system when there are

multiple persons on the floor. The number of targets to be tracked was fixed to two, and two recordings of a person walking on the floor were merged together. In both of these samples, the test subject walked randomly for 3 minutes. The recorded observations of the first sample were merged with the observations from the second sample by shifting the recorded observation times. This arrangement simulates two targets reasonably well, although sometimes the targets pass so close to each other that in reality they would collide.

With multiple targets the tracking problem becomes considerably more difficult. In addition to the state estimation problem, the tracking algorithm has to solve the data association problem, i.e. decide which measurements originate from which targets. While there are many well-known multiple-target tracking (MTT) algorithms described in the tracking literature, such as multiple-hypothesis tracking (MHT) [21], we chose to use a novel algorithm called Rao-Blackwellized Monte Carlo Data Association (RBMCDA), partly because of its elegant theoretical background but mostly because of the ease of implementation using the free RBMCDA Toolbox for Matlab [22].

f. Rao-Blackwellized Monte-Carlo Data Association

RBMCDA is a Rao-Blackwellized sequential Monte Carlo method for tracking multiple targets [23]. Like the Kalman filter, it can be seen as a special case of the Bayesian filtering framework in that it tries to estimate the posterior probability distribution of the system state from noisy measurements using the Bayesian filtering equations. In principle, the algorithm separates the MTT problem into a data association problem, which is solved using a sequential importance resampling (SIR) particle filter, and a state estimation problem, which is solved using a Kalman filter. Furthermore, if the target states are assumed to be independent of each other, the state of each target can be estimated using a separate Kalman filter. In this case the algorithm is quite similar to the MHT algorithm in that it maintains multiple data association hypotheses and evolves the target states using Kalman filters. Nevertheless, it is based on different principles and uses very different methods for maintaining the hypotheses.

We decided to use the same CWNA dynamic model in the multiple target case as we did in the single target case. However, the observation model has to be different – we cannot use the measurement centroids because we do not know the correct measurement associations and hence cannot compute the centroids. Therefore, in the multiple targets case we used the locations of the

active sensors as measurements and simply ignored the strengths of the measurements. This leads to the same observation model as in (6) except for the measurement noise covariance $\mathbf{R}$, which has to be estimated with (9) using the sensor locations instead of the centroids.

e. Multiple target performance analysis

The recorded data of the two targets were run through the RBMCDA algorithm, frame by frame. Each frame was analyzed as a separate trial and was flagged with the number one if the discrimination was a success. The definition of a successful trial was that the NFI observations were associated correctly with the two targets. Those frames where both of the targets activated the same sensor cell at the same time were discarded, because there is no way to determine the owner of that observation.

After the trials, we have a table with ones and zeros indicating the success of each trial, and a table with corresponding gaps between the people. The gap is the distance between their reference locations. To convert these tables into discrimination performance as a function of distance between the targets, we use a histogram and interpolate the desired values from it. The bin width was chosen to be 10 centimeters.

III. EXPERIMENTAL RESULTS

a. Reference Verification

We measured the absolute positioning accuracy of the triangulation reference using ten evenly distributed points on the floor whose locations were well known. The results show that the mean error is 2.53 centimeters, with a 1.13-centimeter standard deviation. An update rate of 50 Hz was also achieved.

Figure 4 illustrates how accurately the system can trace the shape of a complex object in 3D. The figure was created by "painting" the ladder with the node of the three lines.
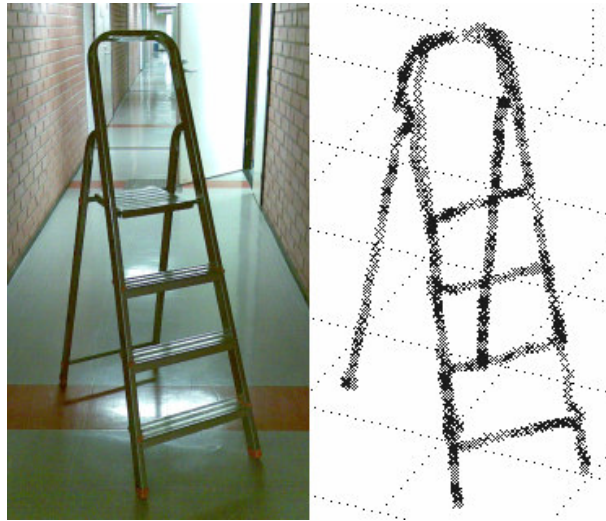
Figure 4. A 3D model of a folding ladder created with the reference system.

b. Positioning Accuracy

One test lap can be seen in figure 5. The mean walking speed was 0.71 m/s and the observation rate was 99.2%. By observation rate we mean the proportion of time during which there are one or more observations of the target available. The black trace shows the reference position, which was acquired with the triangulation system. It shows the position of the head of the test subject. Green circles represent the raw NFI observations, and the gray rectangles represent NFI sensor cells. The blue trace shows the path of the centroid, and the red trace shows the path of the Kalman filter estimate.
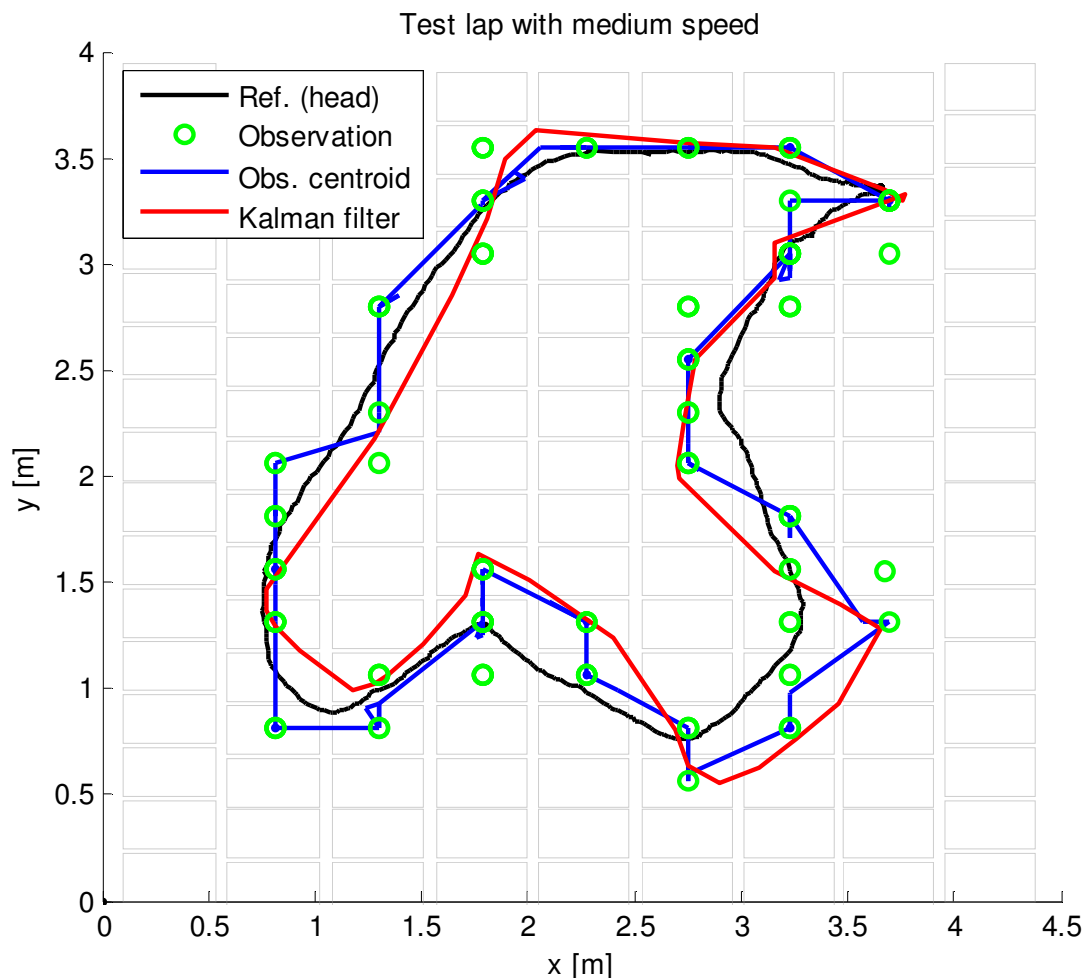
Figure 5. Traces of one test lap. The gray rectangles represent the NFI sensor cells.

Table 1 shows the mean errors categorized by the average walking speeds of the samples. Table 2 presents the corresponding standard deviations of the errors. Observing the tables, one can notice the improvement in accuracy when advancing in the tracking method column. However, the Kalman filter performs poorly in the high-speed samples. The walking speed categories have the following ranges: slow is from 0.33 to 0.47 m/s, medium is from 0.49 to 0.61 m/s, and fast is from 0.66 to 1.06 m/s.

Table 1: Mean errors

Mean error [m]	Walking speed

Tracking method	Slow	Medium	Fast	All
Strongest obs.	0.180	0.192	0.306	0.226
Obs. centroid	0.160	0.177	0.297	0.211
Kalman filter	0.156	0.173	0.306	0.212

Table 2: Standard deviations of errors

S.D. [m]	Walking speed			
Tracking method	Slow	Medium	Fast	All
Strongest obs.	0.100	0.114	0.205	0.140
Obs. centroid	0.095	0.109	0.194	0.133
Kalman filter	0.094	0.106	0.197	0.132

The positioning error of one test subject as a function of walking speed is depicted in figure 6. Walking speeds are averaged within each test walk, as are the errors.
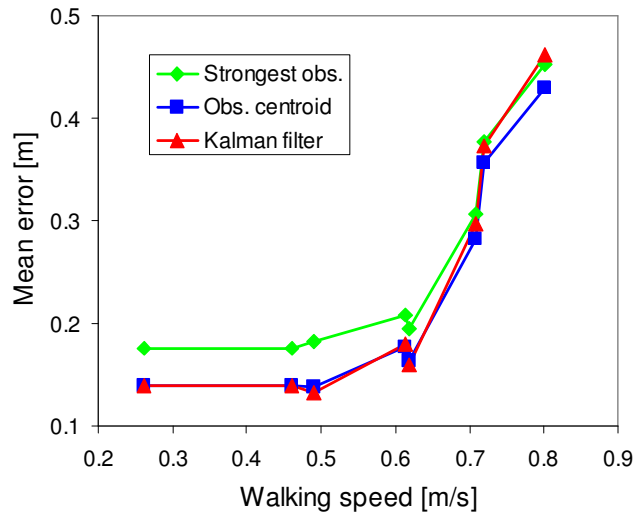
Figure 6. Positioning error of one test subject as a function of walking speed.

The positioning errors of the whole group as a function of observation rate are shown in figure 7. By observation rate we mean the proportion of time during which a target activates at least one

sensor cell while walking alone on the sensor floor. The mean observation rate for the whole group was 91.6%.
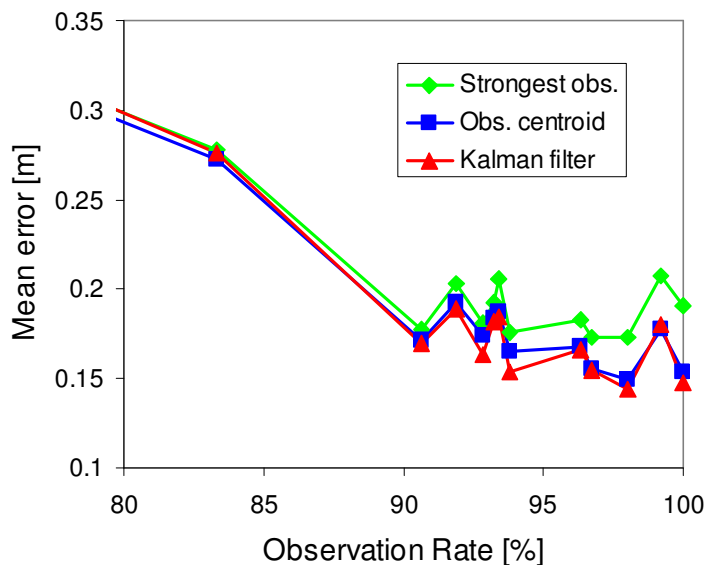
Figure 7. Positioning errors of the whole test group plotted as a function of observation rates.

c. Multi-target discrimination

The RBMCDA discriminates between two people as shown in part a) of figure 8. When the gap R between the two targets is equal to or greater than 110 centimeters, a 99% performance is achieved. A 90% performance is achieved when R is equal to 78 centimeters.

There was some variation between sequential runs of the RBMCDA algorithm, caused by its non-deterministic nature. To cancel this noise, the histogram contains the results of 1200 sequential runs of the discrimination process. There is some residual error caused by the limited sample size and the linear interpolation process, but we believe it to be negligible.

Part b) of figure 8 shows the two merged 3-minute walking samples, which were used for the discrimination performance calculations.
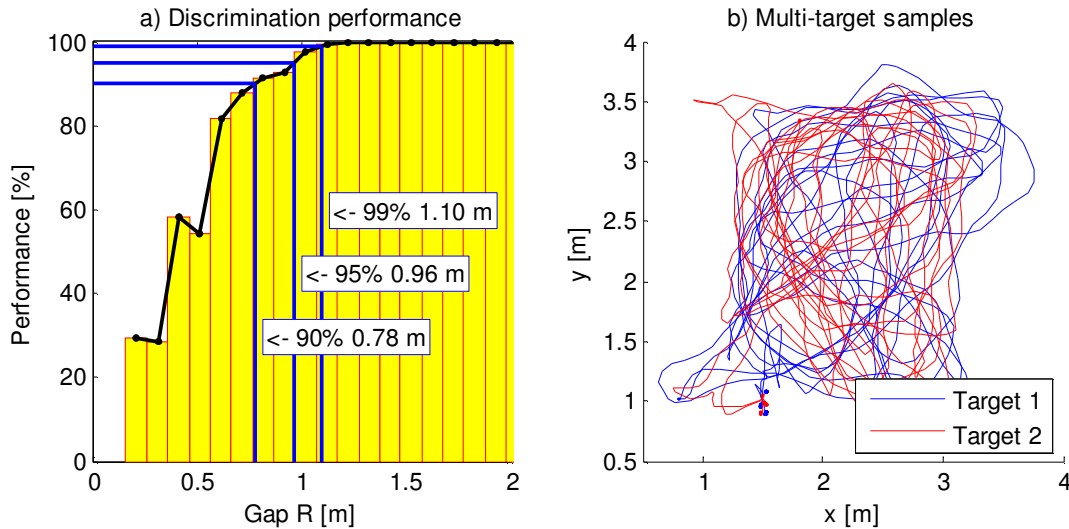
Figure 8. a) RBMCDA discrimination performance of two people as a function of the gap between them. b) The data used in the calculation. Blank areas are caused by furniture.

IV.   DISCUSSION

The unique reference positioning system allowed us to measure positioning errors freely and in real time. Thus we did not have to make such assumptions as the one that the test subject was walking exactly on a predefined route and exactly at a uniform speed. The verification results show that the triangulation reference system is approximately eight times more accurate and ten times faster than the floor sensor system under study. The one-decade goals in these values were nearly reached.

Observing figure 4 suggests that the accuracy of the reference system is more than adequate for the purposes of this study.

b. Positioning accuracy

The positioning accuracy comparison shows that the Kalman estimate outperforms the raw observation and centroid estimates with slow and medium walking speeds. This conclusion is based on the mean error values in Table 1. However, the winning margin of the Kalman filter is not large. Fast walking samples were especially problematic for the Kalman filter because the process noise in the dynamic model was not high enough also to cover the fast walking speed scenario. With fast walking speeds, a simple centroid of observations was the best estimator.

The lowest tracking error was obtained here with the Kalman filter. The mean error was 21.2 centimeters, with a standard deviation of 13.2 centimeters. The use of an SIR particle filter [24] with the same CWNA kinematic model but a more accurate non-linear observation model did not reduce the mean error result significantly and was therefore left out of this study.

Murakita reported a mean tracking error of 20 centimeters using a sensor pitch of 18 x 18 cm [17]. Considering that our sensor cell is almost four times larger (25 x 50 cm), the mean error of 21 centimeters is very competitive. This suggests that linear observation strengths improve accuracy compared to discrete observations.

The results acquired using samples from only one test subject show that the walking speed has a clear effect on the positioning error (see figure 6). This is most probably due to the limited update rate of the floor sensor system, which is approximately 5 updates per second. Some error may also be caused by the attachment point of the triangulation lines, which is located on top of the test subject's head; people tend to lean forward when increasing speed. Figure 6 confirms that the Kalman filter has a slight advantage at slow walking speeds, but at high speeds the CWNA dynamic model is inappropriate and the centroid is the best estimator.

We also noticed a clear relation between lost observations and positioning error, as can be seen in figure 7. It also indicates that the fewer observations the Kalman filter was given, the less competitive it became compared to the simple centroid estimate. Figure 7 includes the entire test group to show the whole spectrum of observation rates. The observation rate depends strongly on the individual characteristics of the test subject, such as walking manner and shoe size. Weight did not seem to have an effect on the observation rate; in fact, the heaviest test subject produced the fewest observations. The 91.6% averaged observation rate of the NFI system was considered to be more than adequate for human tracking purposes.

c. Multi-target discrimination

The discrimination of two targets was implemented using the RBMCDA method with a CWNA dynamic model. The discrimination performance in our study is very similar to the results reported by Murakita [17]. We achieved a 99% discrimination performance with a gap of 1.10 meters, and a 90% performance with a gap of 0.78 meters. The 90% milestone is very competitive compared to the results of Murakita (0.8 m), especially when keeping in mind the disadvantage in our sensor resolution (four times smaller) and the simpler dynamic model. The

RBMCDA method did not use the linear observation strengths, so the good results must be caused by the high observation rates. After all, we do know that Murakita reported a loss of observations while using the discrete floor sensors.

V.   CONCLUSIONS

On the basis of the results, we draw the following conclusions concerning the system under study:

1) using the Kalman filter, the mean tracking error is 21 cm with a standard deviation of 13 cm;

2) the information about the strength of the observations improves positioning accuracy compared to a system with discrete observations;

3) using the RBMCDA for multi-target discrimination, we get 99% success with gaps greater than 1.1 m, and 90% success with 0.8 m.

ACKNOWLEDGMENTS

REFERENCES

[1] H. Rimminen, M. Linnavuo, and R. Sepponen, "Human tracking using near field imaging", Proceedings of the 2dn International Conference on Pervasive Health, Tampere, Finland, Jan. 31-Feb. 2, 2008, pp. 148-151.

[2] T. G. Zimmerman, J. R. Smith, J. A. Paradiso, D. Allport, and N. Gershenfeld, "Applying electric field sensing to human-computer interfaces", pp. 280-287, 1995. [Online]. Available: web.media.mit.edu/~jrs/jrs_EFS_HCI.pdf

[3] H. Rimminen and R. Sepponen, "Biosignals with a Floor Sensor", Proceeding of the. 2nd International Conference on Biomedical Electronics and Devices, Porto, Portugal, 2009, in press.

[4] N. van der Gaag, L. Van Wissen, E. Van Imhoff, and C. Huisman, "National and Regional Population Trends in the European Union. Population and social conditions", Eurostat Working papers, 3/1999/E/n:o 8., 1999, 125 p.

[5] B. G. Celler, W. Earnshaw, E. D. Ilsar, L. Betbeder-Matibet, M. F. Harris, R. Clark, T. Hesketh, and N. H. Lovell, "Remote monitoring of health status of the elderly at home. A multidisciplinary project on aging at the University of New South Wales", International Journal of Bio-Medical Computing, Volume 40, Issue 2, Oct. 1995, pp. 147-155.

[6] M. Alwan, D. C. Mack, S. Dalal, S. Kell, B. Turner, and R. A. Felder, "Impact of Passive In-Home Health Status Monitoring Technology in Home Health: Outcome Pilot", Proceedings of the 1st Transdisciplinary Conference on Distributed Diagnosis and Home Healthcare, 2-4 April 2006., pp.79-82.

[7] A. Ward, A. Jones, and A. Hopper, "A New Location Technique for the Active Office", IEEE Personal Communications, Vol. 4, No. 5, Oct. 1997. pp. 42-47.

[8] R. Want, A. Hopper, V. Falcão, and J. Gibbons, "The active badge location system", ACM Transactions on Information Systems, Vol.10, Issue 1, Jan.1992, pp. 91-102.

[9] H. Cho, M. Kang, J. Park, B. Park, and H. Kim, "Performance Analysis of Location Estimation Algorithm in ZigBee Networks using Received Signal Strength", Proceedings of the 21st International Conference on Advanced Information Networking and Applications Workshops (AINAW'07), 21-23 May 2007.

[10] P. Hii and A. Zaslavsky, "Improving location accuracy by combining WLAN positioning and sensor technology", Workshop on Real-World Wireless Sensor Networks (REALWSN'0), Stockholm, Sweden, June 20-21, 2005.

[11] D. Hihnel, W. Burgard, D. Fox, K. Fishkin, and M. Philipose. "Mapping and localization with RFID technology", Proceedings of the IEEE International Conference on Robotics & Automation, New Orleans, LA, April, 2004. pp. 1015-1020.

[12] S. Jianbo, C. Tomasi, "Good features to track", Proceeding of the IEEE Computer Society Conference on Computer Vision and Pattern Recognition, 1994, pp. 593-600, 21-23 June 1994.

[13]   R. Bodor, B. Jackson, and N. Papanikolopoulos, "Vision-based human tracking and activity recognition", Proceedings of the 11th Mediterranean Conf. on Control and Automation, June 2003.

[14]   M. Addlesee, A. Jones, F. Livesey, and F. Samaria, "The ORL Active Floor", IEEE Personal Communications, Vol. 4, No. 5, Oct. 1997, pp. 35-41.

[15]   R.J. Orr and G.D. Abowd, "The smart floor: a mechanism for natural user identification and tracking", Proceedings of the Conference on Human Factors in Computing Systems (CHI 2000), ACM Press, New York, 2000.

[16]   S. Pirttikangas, J. Suutala, J. Riekki, and J. Roning, "Footstep identification from pressure signals using hidden Markov models", Proceedings of the Finnish Signal Processing Symposium (FINSIG'03), 2003.

[17]   T. Murakita, T. Ikeda, and H. Ishiguro, "Human Tracking using Floor Sensors based on the Markov Chain Monte Carlo Method", Proceedings of the 17th International Conference on Pattern Recognition, 23-26 Aug. 2004.

[18]   R. E. Kalman, "A new approach to linear filtering and prediction problem", Transactions of the ASME – Journal of Basic Engineering, no. 82, Series D, pp. 35-45, 1960.

[19]   B. Ristic, S. Arulampalam, and N. Gordon, "Beyond the Kalman Filter", Artech House, 2004.

[20]   Y. Bar-Shalom, X.R. Li, and T. Kirubarajan, "Estimation with Applications to Tracking and Navigation", Wiley Interscience, 2001.

[21]   S. Blackman and R. Popoli, "Design and Analysis of Modern Tracking Systems", Artech House Radar Library, 1999.

[22]   S. Särkkä and J. Hartikainen, RBMCDA Toolbox for Matlab V1.0, Models and Methods, Centre of Excellence in Computational Complex Systems Research, Helsinki University of Technology, 20 Feb. 2008. [Online]. Available: http://www.lce.hut.fi/research/mm/rbmcda/

[23]   S. Särkkä, A. Vehtari, and J. Lampinen, "Rao-Blackwellized Monte Carlo data association for multiple target tracking", Proceedings of the Seventh International Conference on Information Fusion, Vol. I, 2004, pp. 583-590.

[24]   M.S. Arulampalam, S. Maskell, N.Gordon, and T. Clapp, "A tutorial on particle filters for online nonlinear/non-Gaussian Bayesian tracking", IEEE Transactions on Signal Processing, Vol. 50, No.2, Feb 2002, pp.174-188